Piezoelectric Coefficients of mNA Organic Nonlinear Optical Material Using Synchrotron X-Ray Multiple Diffraction

L. H. Avanci,[1,2,*] L. P. Cardoso,[1] S. E. Girdwood,[3] D. Pugh,[2] J. N. Sherwood,[2] and K. J. Roberts[3]

[1]*Instituto de Física "Gleb Wataghin," Universidade Estadual de Campinas, CP 6165,*
13083-970, Campinas-SP, Brazil
[2]*Pure and Applied Chemistry Department, University of Strathclyde, Glasgow G1 1XL, United Kingdom*
[3]*Centre for Molecular and Interface Engineering, D.M.C. Engineering, Heriot-Watt University,*
Riccarton, Edinburgh EH14 4AS, United Kingdom

Distortions produced in the unit cell of a nonlinear organic crystal under the influence of an applied electric field E are investigated by using synchrotron x-ray multiple diffraction (MD). A typical MD pattern shows numerous (hkl) secondary peaks and the position of each one is basically a function of the unit cell lattice parameters. Thus small changes in any parameter due to a strain produced by E give rise to a corresponding variation in the (hkl) peak position. The method was applied to the meta-nitroaniline (mNA) crystal and we were able to determine three piezoelectric coefficients. [S0031-9007(98)07912-5]

Large high quality noncentrosymmetric organic single crystals have been grown in recent years mainly with the aim of exploiting their nonlinear optical properties, particularly for second harmonic generation and signal modulation via the linear electro-optic effect. The crystals, by virtue of their highly polar, anisotropic structures might also be expected to exhibit substantial piezoelectric and, in some cases, pyroelectric effects, and these responses are related to a range of interesting phenomena, including the optoacoustic and photorefractive effects.

X-ray multiple diffraction (MD) is a technique which has been used by several authors [1–5] to provide a physical solution to the important crystallographic phase problem. Besides, it is closely related to the crystal lattice symmetry which provides three-dimensional information and then is inherently very sensitive to small changes in lattice parameters. A typical single MD pattern shows numerous multiple diffraction peaks, each one carrying information on one particular direction within the crystal. A review of the technique can be found in Ref. [6]. In this paper we present some preliminary results of investigations of the distortions produced in an organic crystal by the application of an electric field. We have measured both multiple and two-beam diffraction peak shifts. The combination of these types of diffraction should provide a versatile method of obtaining complete information on the piezoelectric tensors of crystals of the more anisotropic systems where there are a number of nonequivalent coefficients. The amount of information that can be extracted from one such experimental arrangement is greatly increased if some of the numerous multiple diffraction peaks which appear in a single MD pattern are investigated in addition to the two-beam case.

In the following we discuss the theory relating the piezoelectric distortion of the lattice to the shifts in the diffraction peaks, using as an example one organic non-linear optical crystal mounted in a particular orientation which has been found practicable. Experimental results already obtained are sufficient to establish the feasibility of the technique, as described later on. The organic crystal which has been examined is the meta-nitroaniline (mNA) [7,8] which crystallizes in the orthorhombic system with point group $mm2$ and lattice parameters ($a = 6.501$ Å, $b = 19.330$ Å, $c = 5.082$ Å). The polar axis of the material is **c** [001]. In addition, measurements have been made on lithium niobate [9], which has well established piezoelectric coefficients, in order to assess the reliability of the synchrotron x-ray setup.

The MD phenomenon arises when an incident beam simultaneously satisfies the Bragg law for more than one set of lattice planes within the crystal. A set of planes called primary (h_p k_p l_p) is adjusted to diffract the incident beam. By rotating (ϕ axis) the sample around the primary reciprocal lattice vector, and monitoring the primary intensity, several other planes called secondary (h_s k_s l_s) will also diffract simultaneously with the primary. The interaction between the primary and the secondary reflections is established through coupling reflections (h_p-h_s, k_p-k_s, l_p-l_s) and provides positive (peaks) and negative (dips) features in the pattern $I_{\text{primary}} \times \phi$, called Renninger scan (RS) [10]. The positions of the multiple diffraction peaks in a RS can be measured in terms of the angle, $\beta = \phi^{hkl} \pm \phi_0$ [the signal stands for the entrance and exit of the secondary reciprocal lattice point on the Ewald sphere (ES)], where ϕ_0 is the angle between the secondary vector and the primary incidence plane measured on the ES equatorial plane [11]. This angle is given by

$$\cos(\phi^{hkl} \pm \phi_0) = \frac{1}{2} \frac{(H^2 - \mathbf{H} \cdot \mathbf{H}_0)}{\sqrt{1/\lambda^2 - H_0^2/4}\sqrt{H^2 - H_p^2}},$$

(1)

where $\mathbf{H}_0$ is the primary vector, $\mathbf{H}$ is the secondary vector, $\mathbf{H}_p = (\mathbf{H} \cdot \mathbf{H}_0)(\mathbf{H}_0/H_0^2)$, and λ is the wavelength of the incident beam.

For the orthorhombic mNA crystal, the electric field was applied in the **c** [001] direction and the primary diffraction plane was taken as $(0k_00)$ with $k_0 = 14$. With the secondary chosen as $(h00)$, the magnitudes of the vectors, $\mathbf{H}_0$ and $\mathbf{H}$, defined in the reciprocal lattice, become $H_0 = k_0/b$ and $H = h/a$. In the orthorhombic case these vectors are orthogonal and Eq. (1) reduces to

$$\cos(\phi^{hkl} \pm \phi_0) = h\lambda \frac{b}{a\sqrt{4b^2 - \lambda^2 k_0^2}}. \tag{2}$$

The change in the angle on application of the field can be expressed in terms of the fractional changes induced in the lattice constants by differentiating Eq. (2) to obtain

$$\frac{\Delta a}{a} = \tan(\phi^{h00} \pm \phi_0)\Delta(\phi^{h00} \pm \phi_0)$$
$$- \frac{\lambda^2 k_0^2}{4b^2 - \lambda^2 k_0^2}\frac{\Delta b}{b}. \tag{3}$$

With the secondary chosen as $(00l)$ the analogous formula is

$$\frac{\Delta c}{c} = \tan(\phi^{00l} \pm \phi_0)\Delta(\phi^{00l} \pm \phi_0)$$
$$- \frac{\lambda^2 k_0^2}{4b^2 - \lambda^2 k_0^2}\frac{\Delta b}{b}. \tag{4}$$

A third relation was obtained by measuring the change in the Bragg angle (ω) for the primary diffraction,

$$\frac{\Delta b}{b} = \frac{\Delta d}{d} = -\cot\omega_{\text{Bragg}}^{0k_00}\Delta\omega_{\text{Bragg}}^{0k_00}. \tag{5}$$

The three equations [(3), (4), and (5)] are sufficient to allow the fractional changes in the three orthorhombic lattice parameters to be determined at a given field. In this case the crystal symmetry ensures that a field applied along one of the crystal axes will not induce any changes in the angles between the axes.

When a static or low-frequency electric field is applied to a piezoelectric crystal, strains are developed in the crystal: this is the well-known converse piezoelectric effect. The piezoelectric tensor, expressed in matrix form, for the $mm2$ point group is given by [12]

$$\begin{pmatrix} \varepsilon_{xx} \\ \varepsilon_{yy} \\ \varepsilon_{zz} \\ 2\varepsilon_{yz} \\ 2\varepsilon_{zx} \\ 2\varepsilon_{xy} \end{pmatrix} = \begin{pmatrix} 0 & 0 & d_{31} \\ 0 & 0 & d_{32} \\ 0 & 0 & d_{33} \\ 0 & d_{24} & 0 \\ d_{15} & 0 & 0 \\ 0 & 0 & 0 \end{pmatrix}\begin{pmatrix} E_x \\ E_y \\ E_z \end{pmatrix}, \tag{6}$$

which, with the field applied along the [001] axis, leads to

$$\varepsilon_{xx} = d_{31}E = \Delta a/a, \tag{7a}$$

$$\varepsilon_{yy} = d_{32}E = \Delta b/b, \quad \text{and} \tag{7b}$$

$$\varepsilon_{zz} = d_{33}E = \Delta c/c, \tag{7c}$$

so that the equations above together with Eqs. (3), (4), and (5) allow in principle the simultaneous determination of three piezoelectric coefficients.

The measurements have been carried out at the synchrotron radiation source (SRS) wiggler station 16.3 [13], Daresbury Laboratory, Warrington, U.K. This station is a high-resolution/high-energy single crystal diffraction facility equipped with a Huber 512 diffractometer with servo control providing step sizes of 0.1 and 0.5 mdeg. in ω and ϕ axes, respectively. The wavelengths used in our experiments were 1.2 and 1.4878 Å for measurements in LiNbO$_3$ and mNA, respectively. Figure 1 shows the scheme for applying the electric field in the sample as well as the MD path for one of the measured three-beam cases. The electric field was generated by a variable voltage low current dc power supply. The electric contacts are established through conductive sponges (Fig. 1a), kindly provided by SGL Carbon Group, Meitingen, Germany, placed between the metal plates and the sample larger face which establish a uniform electric field within the crystal. The sponge also avoids mechanical strain in the sample due to physical contact. Typical sample dimensions are 20 mm × 10 mm × 2–5 mm, and the x-ray incident beam hits the narrower sample face allowing for both rocking and RS measurements with the same setup. The samples were prepared by cleaving slices from mNA large high quality single crystals. They were cut in a solvent saw and a first polishing was made by hand in a wet tissue with solvent. The necessary surface degree of flatness and parallelism required was achieved by mechanical polishing.
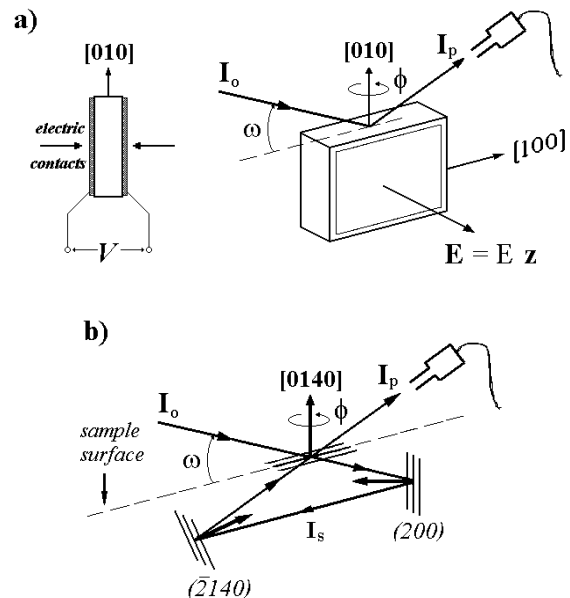

FIG. 1. (a) Scheme for applying the electric field in the sample allowing for both rocking and Renninger measurements with the same setup. The arrows show the sponges for electric contacts. Incident (I_0) and primary (I_p) beam directions, respectively. (b) Possible MD path for the (000) (0140) (200) three beam case in the RS. $(\bar{2}140)$ is the coupling plane and I_s is the secondary beam.
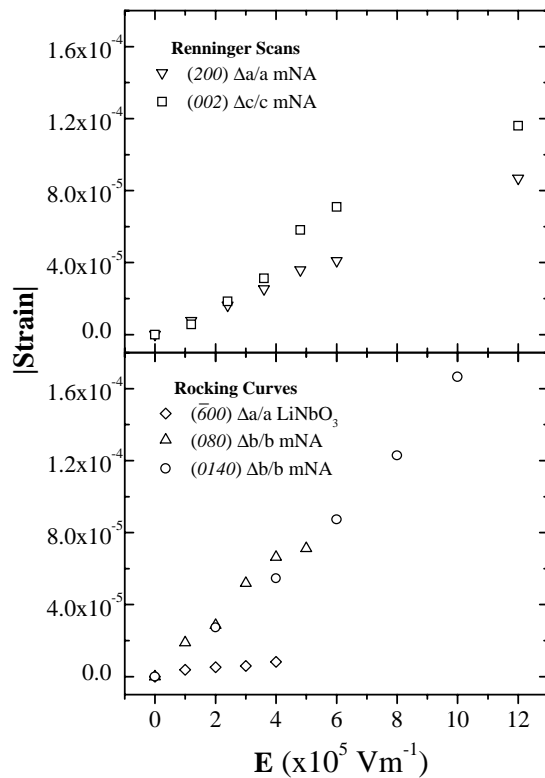
FIG. 2. Plots of the strain $\times E$ for rocking curves and Renninger scans. The piezoelectric coefficients are determined from the slope of the curves.

The results of the application of the field on the rocking curve for the $(\bar{6}\,0\,0)$ primary diffraction peak in $LiNbO_3$ through the peak shifts are shown in Fig. 2.
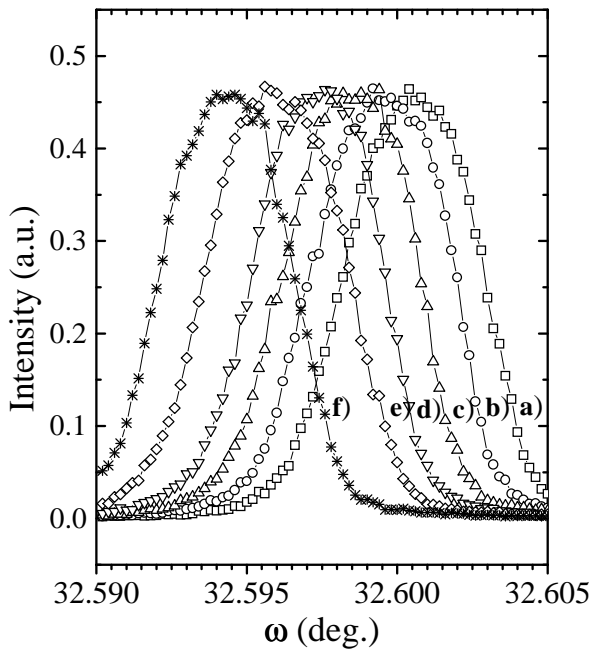

FIG. 3. Change on (0140) rocking curves due to application of the E varying up to 1×10^6 V m^{-1} parallel to the **c** axis. (a) 0 V m^{-1}, (b) 2×10^5 V m^{-1}, (c) 4×10^5 V m^{-1}, (d) 6×10^5 V m^{-1}, (e) 8×10^5 V m^{-1}, and (f) 10×10^5 V m^{-1}.

From the slope of the curve $\Delta b / b \times E$ the value of $|d_{22}| = 1.9(3) \times 10^{-11}$ m V^{-1} piezoelectric coefficients is determined. Figure 2 shows this curve together with all other curves determined in this work. This value lies within the range obtained in previous reported measurements [14].

Several rocking curves for mNA were obtained in the absence of the electric field, for two primary reflection (080) and (0140). The shape and reproducibility shows that the crystal quality and the experimental setup can provide the determination of very small changes in lattice parameters. Figure 3 shows how the (0140) rocking curves change on application of the electric field up to 1×10^6 V m^{-1} parallel to the **c** axis. It can be seen that the shapes of the curves are undistorted and that a clearly defined shift in the peak position can be measured. These features are a clear evidence of the lattice strain produced by the piezoelectric effect. From the slope of $\Delta b / b$ [Eq. (5)] $\times E$ plotted in Fig. 2, we can obtain $|d_{32}| = 16.5(7) \times 10^{-11}$ m V^{-1}. An analogous procedure varying the electric field up to the 5×10^5 V m^{-1}, the (080) rocking curve measurements have provided $|d_{32}| = 14.9(5) \times 10^{-11}$ m V^{-1} which confirms the previous result. After the measurement of a complete E cycle the peak position has returned to its initial position, indicating the reversibility feature of the E effect to the mNA lattice [15].
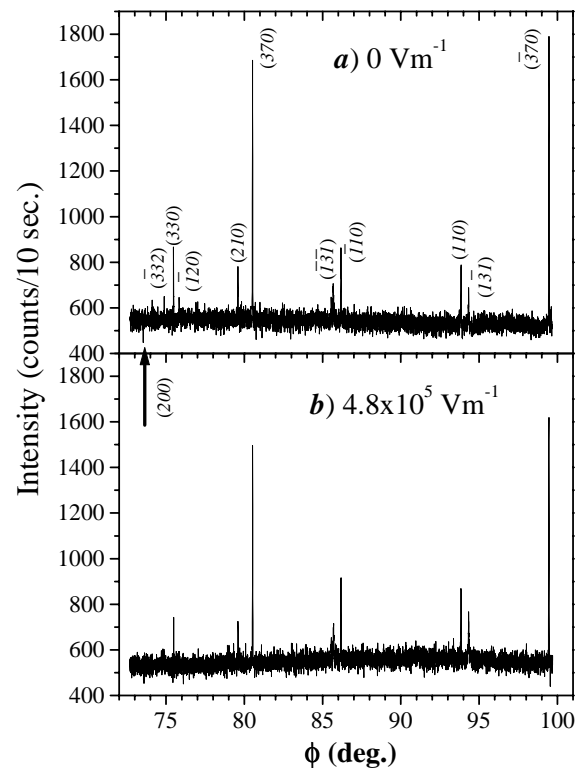

FIG. 4. Region around the $\phi = 90$ deg. symmetry mirror of the mNA (0140) RS without (a) and with (b) an 4.8×10^5 V m^{-1} electric field applied. The various secondary peaks appear indexed for a clear identification of the symmetry mirror. Radiation CuK$_{\alpha 1}$ ($\lambda = 1.540\,56$ Å); step size: 2 mdeg.
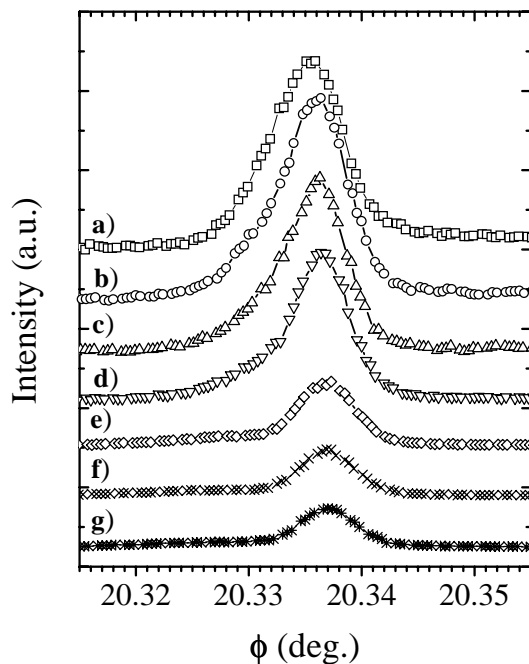
FIG. 5. Changes on the three-beam (000) (0140) (002) peak position in the RS with the application of $\mathbf{E} \parallel \mathbf{c}$. (a) 0 V m^{-1}, (b) $1.2 \times 10^5 \text{ V m}^{-1}$, (c) $2.4 \times 10^5 \text{ V m}^{-1}$, (d) $3.6 \times 10^5 \text{ V m}^{-1}$, (e) $4.8 \times 10^5 \text{ V m}^{-1}$, (f) $6 \times 10^5 \text{ V m}^{-1}$, and (g) $12 \times 10^5 \text{ V m}^{-1}$.

The two-beam data could be supplemented by measurements of multiple diffraction peaks. Figure 4 shows the region around the $\phi = 90$ deg. symmetry mirror of the mNA (0140) RS without (Fig. 4a) and with (Fig. 4b) an $4.8 \times 10^5 \text{ V m}^{-1}$ electric field applied, for comparison purposes. The various secondary peaks appear indexed for a clear identification of the mirror symmetry. Apart from the small intensity changes due to the E induced strain, the lattice symmetry is preserved under E action. From the whole RS we choose the secondary reflections (200) and (002) since they are directly related to the lattice strains $\Delta a/a$ and $\Delta c/c$. These reflections, as described in the theory, allow for the determination of the two other piezoelectric coefficients d_{31} and d_{33}. The three-beam case involving the (000) incident, (0140) primary, and (002) secondary reflections, appearing at $\phi = 20.335$ deg., was measured from RS with several E values increasing up to $1.2 \times 10^6 \text{ V m}^{-1}$. The shift in the (002) peak position as a function of E is shown in Fig. 5. Equations (4) and (5) allow the plot of $\Delta c/c \times E$ curve also depicted in Fig. 2, from which $|d_{33}| = 10.3(8) \times 10^{-11} \text{ m V}^{-1}$ is determined. An analogous procedure for the three-beam case (000) (0140) (200), $\phi = 74.237$ deg. [Fig. 1b], using now Eqs. (3) and (5) gives rise to $|d_{31}| = 7.3(1) \times 10^{-11} \text{ m V}^{-1}$. In Fig. 5 the secondary peak intensity decreases due to the effect of E in the exact Bragg diffraction condition for the primary planes (cell distortion). Regarding the results of mNA piezoelectric coefficients, $|d_{31}|$, $|d_{32}|$, and $|d_{33}|$ are bigger than those obtained via the direct effect in

Ref. [16], since electrode-area effects in soft polymeric materials can cause systematic difference between the direct and inverse piezoelectric coefficients [17]. All three coefficients determined in this work present the same order of magnitude of the elastic constants in the corresponding directions for the same material as suggested elsewhere [18]. It is also important to stress the linearity obtained in all strain $\times E$ plots including that for LiNbO$_3$ shown in Fig. 2, as expected from the piezoelectric effect.

The results obtained show that the response of polar organic crystals in the application of an electric field can be monitored by a combination of two beam and multiple x-ray diffraction techniques. The results described are not intended as accurate determinations of piezoelectric coefficients, but are presented as evidence that this kind of application of the multiple diffraction technique can provide a useful extension of experimental method when the anisotropy of the crystal response is such as to require measurements of a number of tensor material coefficients.

*Email address: lhavanci@ifi.unicamp.br

[1] M. Hart and A. R. Lang, Phys. Rev. Lett. **7**, 120 (1961).
[2] R. Colella, Acta Crystallogr. Sec. A **30**, 413 (1974).
[3] B. Post, Phys. Rev. Lett. **39**, 760 (1977).
[4] S. L. Chang, Phys. Rev. Lett. **48**, 163 (1982).
[5] Qun Shen, Phys. Rev. Lett. **80**, 3268 (1998).
[6] S. L. Chang, in *Multiple Diffraction of X-ray in Crystals,* Solid State Science Series Vol. 50 (Springer-Verlag, Berlin, 1984).
[7] A. C. Skapski and J. L. Stevenson, J. Chem. Soc. Perkin Trans. **2**, 1197 (1973).
[8] J. G. Bergman and G. R. Grane, J. Chem. Phys. **66**, 3803 (1977).
[9] Kindly provided by H. Gallagher from the Optical Materials Research Centre, Phys. and Appl. Phys. Dept., University of Strathclyde, Glasgow, U.K.
[10] M. Renninger, Z. Phys. **106**, 141 (1937).
[11] H. Cole, F. W. Chambers, and H. M. Dunn, Acta Crystallogr. **15**, 138 (1962).
[12] J. F. Nye, in *Physical Properties of Crystals* (Clarendon Press, Oxford, 1985).
[13] S. P. Collins, R. J. Cernik, C. C. Tang, N. W. Harris, M. C. Miller, and G. Oszlanyi, J. Synchrotron Radiat. **5**, 1263 (1998).
[14] R. S. Weis and T. K. Gaylard, Appl. Phys. A **37**, 191 (1985).
[15] L. H. Avanci, R. S. Braga, L. P. Cardoso, D. S. Galvão, D. Pugh, and J. N. Sherwood (to be published).
[16] A. L. Bain, N. El-Korashy, S. Gilmour, R. A. Pethric, and J. N. Sherwood, Philos. Mag. B **66**, 293 (1992).
[17] S. C. Abrahams, Acta Crystallogr. A **50**, 658 (1994).
[18] C. S. Yoon, Ph.D. thesis, University of Strathclyde, Glasgow, U.K., 1986.